Journal of Korean Association of Crystal Growth
Vol. 9, No. 5 (1999) 454-458

Modelling of transport phenomena and meniscus shape in Czochralski growth of silicon material

Sun Hyuk Bae, Jong Hoe Wang* and Do Hyun Kim
Department of Chemical Engineering, KAIST, Taejon 305-701, Korea
**R&D Center, LG Siltron Inc., Kumi 730-350, Korea*
(Received June 9, 1999)

Abstract Hydrodynamic Thermal Capillary Model developed previously has been modified to study the transport phenomena in the Czochralski process. Our analysis is focused on the heat transfer in the system, convection in the melt phase, and the meniscus and interface shape. Four major forces drive melt flow in the crucible, which include thermal buoyancy force in the melt, thermocapillary force along the curved meniscus, crucible rotation and crystal rotation. Individual flow mechanism due to each driving force has been examined to determine its interaction with the meniscus and interface shape. A nominal 4-inch-diameter silicon crystal growth process is chosen as a subject for analysis. Heater temperature profile for constant diameter crystal is also presented as a function of crystal height or fraction solidified.

1. Introduction

The Czochralski crystal growth technique is the most widely used method for producing large single crystals of silicon for use as substrates in the fabrication of electronic devices. The understanding of transport phenomena in Czochralski process is prerequisite to optimize the system for the control of crystal quality. There have been many models proposed to solve the transport equations in Czochralski silicon growth.

In the Czochralski method single crystal is pulled vertically from the surface of a heated pool of melt contained in a cylindrical crucible. Resistance heating is typically used for semiconductor material and inductive heating is common for oxide material with higher melting point. Growth is initiated by lowering a small seed crystal to the surface of the melt pool to give the desired orientation of crystal. After thermal equilibration of the seed with the melt, the seed is raised and the temperature of the melt is lowered to induce growth of the crystal. By the control of the thermal environment and pulling rate, the crystal radius is increased to a desired value and then kept constant afterwards [1-3].

In this study, Hydrodynamic Thermal Capillary Model developed by Sackinger [4] was modified to study the heat transfer process, convection in the melt, and the shape of free boundaries in Czochralski silicon crystal growth. Four major driving forces for melt flow in the crucible are thermal buoyancy force in the melt, thermocapillary force along the curved meniscus, crucible rotation and crystal rotation. Individual flow mechanism due to each driving force is examined to determine its interaction with the free boundaries in the Czochralski growth configuration. Parameters in a nominal 4-inch diameter silicon crystal growth process are used in our study.

2. Modelling

The geometry of the mathematical model for Czochralski process for the growth of semiconductor materials is shown schematically in Fig. 1. The multiple domains represent different physical regions of the system: crystal (s), melt (m), quartz liner (l) and crucible (c), each of which is characterized by different thermophysical properties. The cylindrical coordinate system (r, z) is centered at the bottom of the crucible and the unknown boundary shapes are h_o and h_l for the melt/crystal interface and the melt/ambient meniscus, respectively. In this analysis, the radius of cylindrical crystal is assumed to be constant, but its value is not set *a priori* and calculated as a part of the solution. The temperature has been scaled with the absolute melting temperature and the lengths with the inner radius of the crucible/liner assembly. Growth parameters for HTCM simulations are listed in Table

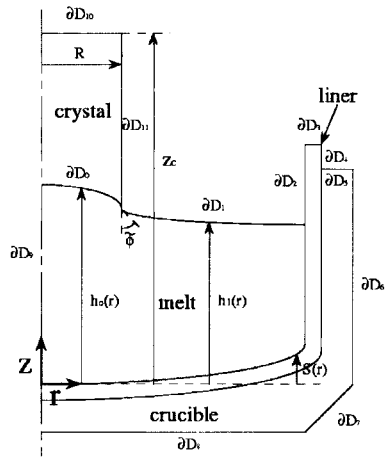

Fig. 1. Schematic diagram of domains for the mathematical model and free surfaces.

Table 1
Growth parameters for HTCM simulations

Symbols	Meaning/definition	Values
$\tilde{M}_0$	Initial mass of starting material	25 kg
$\tilde{z}_c$	Top position of grown crystal	30 cm
$\tilde{R}_c$	Inner radius of crucible	14.395 cm
$\tilde{R}_{set}$	Setting of crystal radius	5.3 cm
$\tilde{T}_{aT}$	Ambient temp. of top side	900 K
$\tilde{T}_{aB}$	Ambient temp. of crucible bottom	1,500 K
$\tilde{V}_g$	Growth rate of crystal	0.5 mm/min
σ	Stephan-Boltzmann constant	5.7×10^{-12} W/cm^{2}K^4
$\tilde{\beta}_m$	Thermal expansion coefficient	1.4×10^{-4} K^{-1}
$d\tilde{\gamma}/d\tilde{T}$	Thermocapillary coefficient	0.43 dyne/cm · K
$\tilde{\omega}_s$	Crystal rotation rate	10 rpm
ω_c	Crucible rotation rate	-8 rpm

1. Dimensionless groups are listed in Table 2.

The quasi-steady state (QSS) approximation is used to construct the hydrodynamic thermal capillary model (HTCM). The effect of the *batchwise decrease of the melt volume* is accounted using the mass balance of melt and crystal from the initial charge of silicon. The symbols with tilde are used to denote the dimensional quantities. The quasi-steady state model treats the crystal radius as an unknown which is determined as part of the solution. In this model, an augmented equation, setting the radius of crystal to the set value, is used to find the heater temperature consistent with the given crystal radius R_{set}.

Table 2
Dimensionless groups appearing in the HTCM

Symbols	Definition	Name/Description
Pr	$\tilde{\nu}_m/\tilde{\alpha}_m$	Prandtl number
Pe	$\tilde{V}_g\tilde{R}_c/\tilde{\alpha}_s$	Peclet number for heat transfer in crystal
St	$\Delta\tilde{H}_f/\tilde{C}_{p,s}\tilde{T}_m$	Stefan number
Ra	$\tilde{g}\tilde{\beta}_m\tilde{T}_m\tilde{R}_c^3/\tilde{\alpha}_m\tilde{\nu}_m$	Rayleigh number
Ma	$(d\tilde{\gamma}/d\tilde{T})\tilde{T}_m\tilde{R}_c/\tilde{\rho}_m\tilde{\alpha}_m\tilde{\nu}_m$	Marangoni number
Re_s	$\tilde{\Omega}_s\tilde{R}_c^2/\tilde{\nu}_m$	Rotational Reynolds number for crystal
Re_c	$\tilde{\Omega}_c\tilde{R}_c^2/\tilde{\nu}_m$	Rotational Reynolds number for crucible

Our analysis incorporates the free boundaries inherent to the Czochralski system with the heat transfer calculation. The shapes of the melt/crystal interface and melt/ambient meniscus and the radius of crystal are determined simultaneously with the temperature field throughout the system. The details of the model can be found in the accompanying paper [5].

HTCM accounts the effects of dynamic pressure and viscous stress on the shape of the melt/gas interface. The fluid flow interacts with the shape of the melt/crystal interface and crystal radius as the convection and the temperature field affects each other. The conditions on the boundaries between regions guarantee that temperature is continuous and energy is conserved across boundaries. At the melt/crystal interface (∂D_0), latent heat is released on solidification and accounted in the boundary condition across the interface.

Complete set of partial differential equations, boundary conditions and constraints defines a nonlinear multiple free-boundary problem for the i) temperature field in the melt, crystal, liner and crucible, ii) the melt convection in the melt, iii) the shape of melt/crystal interface and melt/ambient meniscus, iv) the melt volume, v) the heater temperature and vi) the crystal height. Whole problem is solved using finite element method with biquadratic basis function for the velocity and temperature and discontinuous linear basis function for the pressure field. Melt/crystal interface and meniscus are mapped isoparametrically using quadratic basis functions.

The velocity field for all calculations is displayed in terms of the stream function, ψ, calculated with the condition of $\psi = 0$ along the boundaries of the melt phase.

3. Result and discussion

Computations were performed using the mesh shown in Fig. 2. The isotherms and interface shapes for conduction dominated case using HTCM with all flow mechanisms suppressed are shown in Fig. 3.

Computer simulations were performed to understand the heat transfer and convection in the Czochralski system and to test the influence of convection in the melt on the melt/crystal interface shape. Four driving forces for convection in the melt are decoupled in the analysis to investigate the effect of each flow mechanism. These are buoyancy-driven convection, thermocapillary motion, crucible rotation and crystal rotation.

The flows driven by the different mechanisms for convection are shown in Fig. 4-7.

In each case, the growth conditions listed in Table 1 are used for the calculation with other flow mechanisms suppressed. Contours are shown for the temperature field throughout the system, the stream lines and the azimuthal velocity u_θ. The dotted line at the contours of the stream lines represents the negative value, which indicates that the flow direction is reversed. The results of mixed convection including all flow mechanisms are shown in Fig. 8.

In the mixed convection case, where all the flow mechanisms are accounted, the temperature field becomes more complex than the case with any other individual flow mechanism. But, the temperature field in the vicinity of crystal is nearly same as in the case with buoyancy driven convection. For the melt flow, the flow beneath the crystal maintains the flow as in

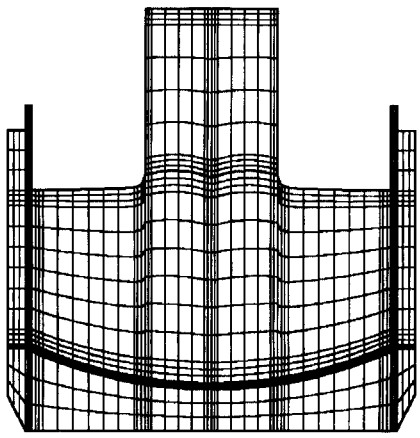

Fig. 2. Sample mesh shapes used in the calculation of HTCM.

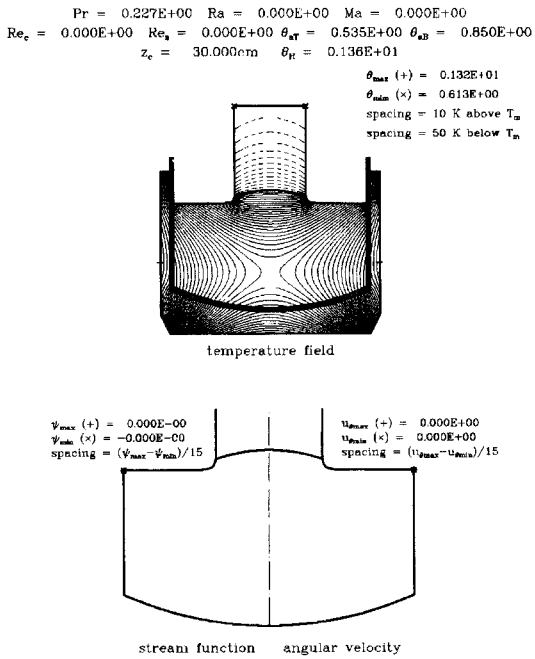

Fig. 3. Interface shapes and contours of temperature, stream function and azimuthal velocity for no convection with conduction only.

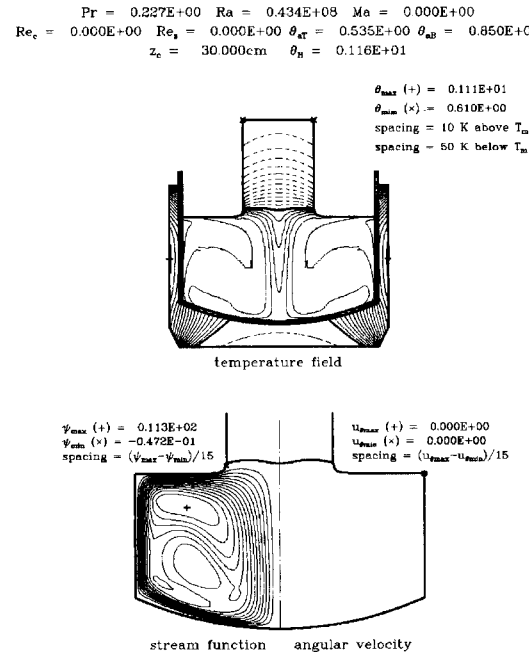

Fig. 4. Interface shapes and contours of temperature, stream function and azimuthal velocity for buoyancy-driven convection.

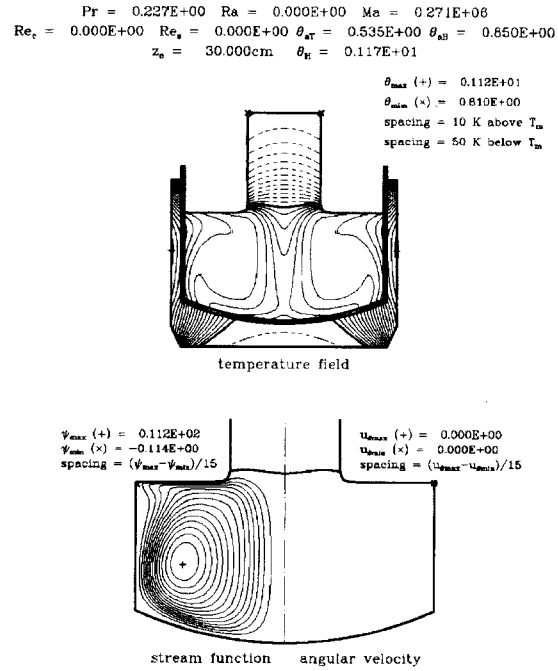

Fig. 5. Interface shapes and contours of temperature, stream function and azimuthal velocity for thermocapillary convection.

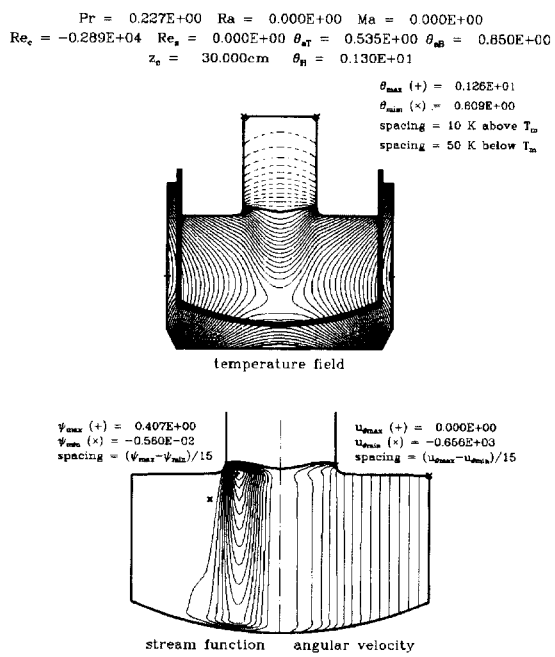

Fig. 6. Interface shapes and contours of temperature, stream function and azimuthal velocity with crucible rotation.

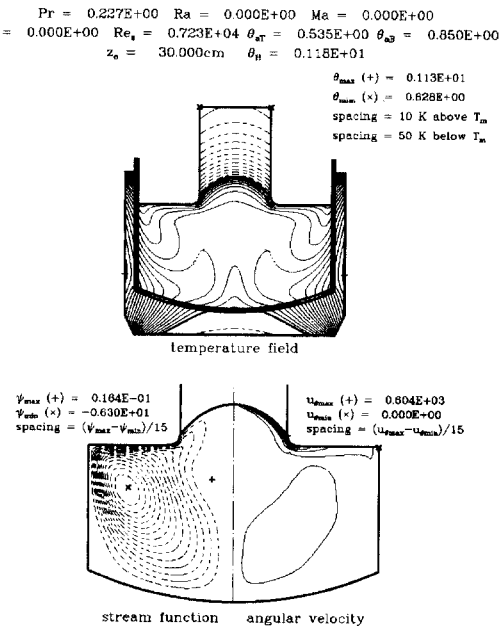

Fig. 7. Interface shapes and contours of temperature, stream function and azimuthal velocity with crystal rotation.

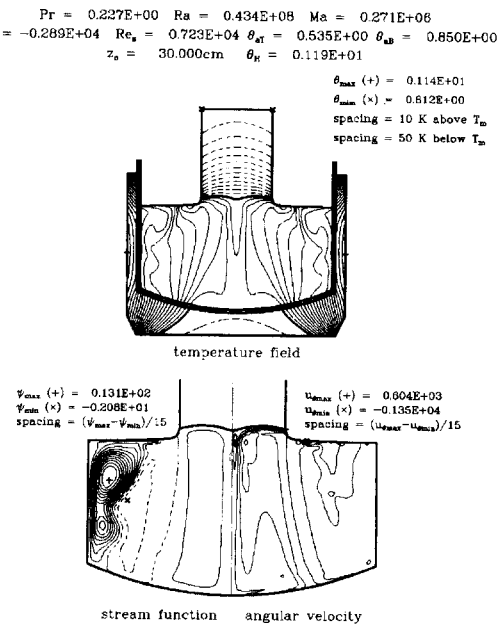

Fig. 8. Interface shapes and contours of temperature, stream function and azimuthal velocity for mixed convection.

the case of crucible rotation although it is weak. The intense flow occurs outside the crystal near the cruci-

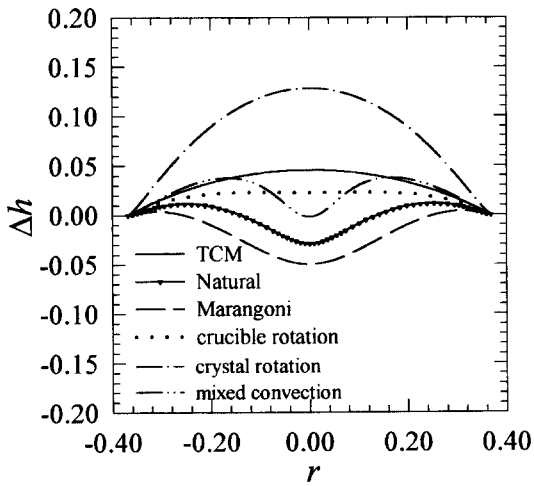

Fig. 9. Relative melt/crystal interface shapes.

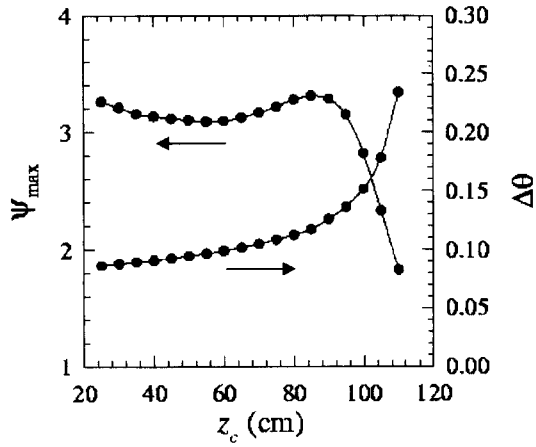

Fig. 10. Heater temperature and maximum stream function value as a function of crystal top position (Pr = 5, all flow mechanisms are included).

ble wall, which is a mixed flow of buoyancy driven convection and thermocapillary convection. But, the flow structure has two cell structure as in the case of buoyancy driven convection. Between these regions, melt flow seems to be driven by the crystal rotation.

The melt/solid interface shape is sensitive measure of the heat flow in that area and important to *radial* segregation. The melt/crystal interface shapes plotted in Fig. 9 demonstrate the relative melt/crystal interface shape under various flow mechanisms. Since the buoyancy driven convection is the dominant flow mechanism, the interface shape in the mixed convection is similar to the one with buoyancy-driven convection. Interface shape in mixed convection agrees qualitatively with the gull-winged interface shape observed experimentally by Kinney and Brown [6]. They used X-ray transmission topography with a longitudinal section of a 4-inch crystal.

During the crystal growth process, the volume of the melt slowly decreases. We have changed the crystal top position to study the effect of the change of melt volume shown in Fig. 10. Heater temperature should increase as the crystal top position increases and the depth of melt decreases. This is because more heat lost through the crystal should be supplied to maintain the constant radius of the crystal. The maximum stream function indicating the intensity of flow decreases as the depth of melt decreases because the buoyancy driven convection is scaled with the cube of length scale as in the Rayleigh number. Although the length scale in the Rayleigh number is the inner radius of the crucible, the depth of melt has almost same influences.

4. Conclusions

Nominal 4-inch Si crystal growth system has been simulated numerically. Each flow mechanism was decoupled in the analysis and compared to the case with all four mechanisms, to examine the effect of convection on the interface shape and to determine the dominant mechanism in the melt flow. The case with mixed convection shows that the melt flow depends on all the flow mechanisms but the buoyancy-driven convection dominates the melt flow. Consistently, the melt/crystal interface shape in the mixed convection case is similar to that in the case with buoyancy-driven convection.

References

[1] J.C. Brice, Crystal Growth Process, (John Wiley & Sons, New York, 1986) p. 129.
[2] J.J. Derby, R.A. Brown, F.T. Geyling, A.S. Jordan and G.A. Nikolakopoulou, J. Electrochem. Soc. 470 (1985) 132.
[3] R.A. Brown, J. Comput. Phys. 33 (1979) 217.
[4] P.A. Sackinger, Flows and Transitions during Solidification: (I) Mode Expansion Calculations of Rayleigh-Bernard Convection in a Cylinder (II) Simulation of Hydrodynamics, Heat Transfer and Free Boundaries in Czochralski Growth, Ph. D. Thesis, (M. I. T., Cambridge, 1989) p. 136.
[5] S.H. Bae, J.H. Wang and D.H. Kim, J. Crystal Growth, Submitted (1999).
[6] T.A. Kinney and R.A. Brown, J. Crystal Growth 132 (1993) 551.